Chapter 6

Electric-driven Zonal Hydraulics in Non-Road Mobile Machinery

Tatiana A. Minav, Jani E. Heikkinen and Matti Pietola

Additional information is available at the end of the chapter

http://dx.doi.org/10.5772/61793

Abstract

The goal of this research is to apply direct-driven hydraulics (DDH) to the concept of zonal (i.e., locally and operation-focused) hydraulics, which is an essential step in the hybridization and automation of machines. DDH itself aims to combine the best properties of electric and hydraulic technologies and will lead to increased productivity, minimized energy consumption and higher robust performance in both stationary and mobile machines operating in various environments. In the proposed setup, the speed and position control of a double-acting cylinder is implemented directly with an electric motor drive in a closed-loop system without conventional control valves and an oil tank. The selection of the location of the hydraulic accumulator and connection of the external leakage lines will also be part of this study. Simulations and experimental research to study the details of the hydromechanical and electrical realization of the DDH are performed.

Keywords: direct driven hydraulics, non-road mobile machinery, energy efficiency, electric drive, hybrid topology, energy regeneration

1. Introduction

The climate for industrial and economic growth is changing as resource scarcity pushes up costs, and enterprises are more closely scrutinized because of changing expectations about their public and social responsibilities. Governments have set tight CO_2 emission rules [1] and new exhaust limits have just been implemented, such as Tier Emission Standards. The next known step will be the 2019/2020 Tier V, which is a regulation imposing an ulterior sharp tightening of exhaust limits, especially in terms of particles. Now, there is a four-year time window to prepare engines for the upcoming regulations through solutions for peak power shaving and the downsizing of diesel engines. Electric and hybrid vehicles are a suitable solution for reaching these target environmental requirements; such vehicles have a huge

potential for application in the non-road mobile machinery (NRMM) industry, with its market in mining, process and goods manufacturing, forest harvesting and construction work. Figure 1 illustrates typical examples of NRMMs.

Figure 1. Examples of non-road mobile machinery: (a) excavator; (b) mine loader and (c) forest harvester.

The NRMM industry and its customers are traditionally quite conservative in putting new ideas and technologies into use. When they opt for "mild hybridization", the machine manufacturers do not need to change the construction frame of the whole machine immediately. However, some changes in layout design concepts, machine types and business models should be considered in the long term. Therefore, we address several challenges to improve NRMMs by bringing zonal hydraulics into machines. Combining the best properties of traditional hydraulics and electric intelligence allows the following benefits to be achieved in NRMMs:

- easy electrification of NRMMs
- higher efficiency compared to conventional machines
- electrohydraulic power pack with no tank and pipelines
- reduction of potential leakage points
- power-on-demand control
- sensorless position control

1.1. State of the art

During recent years, the NRMM industry has had a tendency towards integrated, compact electrohydraulic systems that deliver powerful, linear movement with either valve- or pump-controlled systems. These technological steps are considered important stages towards a solution to commonly identified problems, such as the reduction of CO_2 emissions and improved performance, productivity, reliability and controllability [2, 3], as well as good options for forcing a smaller diesel engine to operate within its optimum efficiency area since, in general, the diesel engines of NRMMs operate far from their optimum efficiency range [4]. Restrictive environmental regulations are not the only factor imposing the need for innovation in NRMMs. Today, as the search for natural resources expands to areas previously considered

http://dx.doi.org/10.5772/61793

too remote and environmentally hostile to support viable extraction and processing operations, researchers all around the world are facing the challenge of establishing and maintaining industrial activities in extreme environments. In these, components of the drive face thermal issues, primarily at start-up, when everything in the drive has cooled down to low, even Arctic temperatures. Under these conditions, conventional hydraulic fluid in all hydraulic systems solidify, so when the NRMM starts up, there is no fluid circulating to protect the pump and other components from extreme wear. For successful operation, a relevant start-up procedure is crucial, as the risk of equipment failure is unacceptable in remote locations.

Zonal or decentralized hydraulics—as we will call it—is an approach first introduced in the aircraft industry [5]. Adapting this time-proven design from the aircraft industry, simplifying its design as well as broadening its orientation and performance options will support a similar development in NRMMs. In a fully zonal system, the hydraulic pumps are removed from the engine and replaced within hydraulic power packs distributed throughout the NRMM system. In this architecture, multiple hydraulic power sources may be utilized in each zone in order to achieve energy savings and work with a power-on-demand approach.

Figure 2 illustrates the zonal hydraulic architecture applied to NRMMs. A challenge in this is the increasing number of electric components in the limited volume available in the vehicle. On the other hand, the main advantages of this architecture are the reduced hydraulic tubing (tubes are replaced with wiring), the elimination of some hydraulic components and simplified machine assembly.

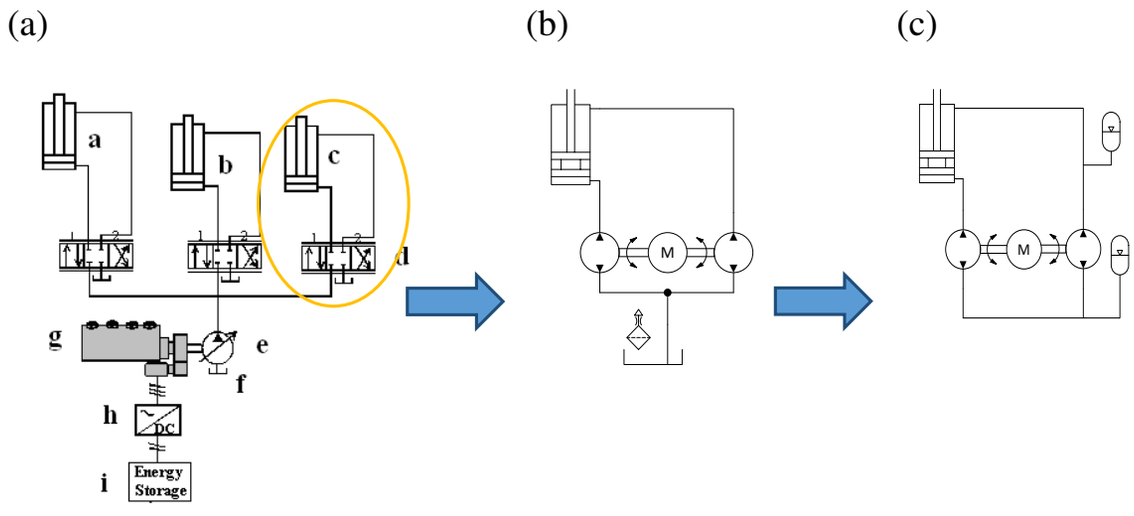

Figure 2. Schematics of (a) conventional NRMM, (b) hybrid NRMM with secondary power source DDH with a conventional tank and (c) DDH without a tank.

In this study, an electrohydraulic actuator (EHA) will be used to achieve high power density, low noise and high performance in a compact package in order to take the development of a power unit onto the next level. The electrohydraulic actuator allows decoupling from the main hydraulic system, thus enabling a zonal approach and, at the same time, reducing parasitic losses in order to obtain better fuel efficiency and lower operating costs. The robust, leak-free,

one-piece housing design delivers system simplicity and lowers both installation and maintenance costs. The electrohydraulic actuator reduces space and weight demands. It can eliminate hoses, fittings, valves and fixtures and is easy to integrate into larger systems.

Currently, electrohydraulic actuators are mostly installed and developed for aircraft applications [6, 7], where the price level and reliability requirements are very high. Most of the research studies related to electrohydraulic actuators have been conducted to adjust the state of the servo valve [8, 9]. However, this approach results in low energy efficiency because of the flow via the pressure relief valves of the hydraulic pumps and throttle losses at the control valves. Consequently, several techniques have been developed to overcome this drawback in order to achieve higher efficiency. In ref. [10], the concept of a pump-controlled electrohydraulic actuator is introduced as an advanced hydraulic system where the proposed structure of the electrohydraulic actuator is directly operated by a bidirectional pump. There are already commercially integrated power packages on the market, but they are based on conventional technology and they do not respond to the above-mentioned challenges created by the hybridization problem. Examples of commercial pump-controlled electrohydraulic actuators are, for instance, the mini-motion package from Kayaba Industry Co. [11] and the intelligent hydraulic servo drive-pack from Yuken Kogyo Co. [12]. The disadvantages of the architecture evidenced in ref. [10] are the use of complex and expensive pumps and the lower dynamic properties of the system in general. In addition, none of these commercial solutions are designed for power-on-demand control, sensorless positioning or even energy regeneration, all highly desirable improvements in a competitive product.

Some studies have been conducted to introduce the concept of electrohydraulic actuators as zonal hydraulics in NRMM. In ref. [13], an electrohydraulic actuator is used for the power steering of heavy vehicles. In refs. [14–17], a compact drive for automation of all kinds of linear motions was introduced and investigated from the thermal point of view. In these sources, even if they proposed direct pump control similar to the direct-driven hydraulic approach, a set of valves is used to balance the flow and to ensure the direction of the electrohydraulic actuator motion. In refs. [18, 19], direct-driven hydraulics (DDH), an electrohydraulic actuator, was introduced without conventional directional valves. The DDH drive combines the best properties of electric and hydraulic drive technologies in one:

- direct control of flow, as well as the velocity and position of the actuator
- high hydraulic efficiency because there are virtually no flow-restricting valves
- no need for expensive variable displacement pumps
- easier to find the optimum operational point for each of the powertrain components (fewer compromises) since each actuator has two pump units and an electric motor
- the pump units and internal combustion motor are disconnected
- possibility of realizing efficient energy recovery systems using both hydraulic accumulators and electric batteries

Therefore, the idea of implementing the DDH drive in the powertrain of NRMMs as an application of the zonal hydraulic concept was born. In this research, direct-driven hydraulics

http://dx.doi.org/10.5772/61793

(DDH) is seen as a tool to convert existing NRMMs to hybrids combining the best properties of traditional hydraulics and electric intelligence. Figure 3 illustrates the hybrid proposal for NRMMs. With this approach, several challenges that traditionally manifest themselves in the hybridization process will be solved. In the proposed setup, the speed and position control of a double-acting cylinder is implemented directly with a motor drive in a closed-loop system without conventional control valves and an oil tank. The selection of the optimal size and the location of the hydraulic accumulator will also be part of this study. Simulations and experimental research to study the details of the hydro-mechanical and electrical realization of the DDH will be performed.

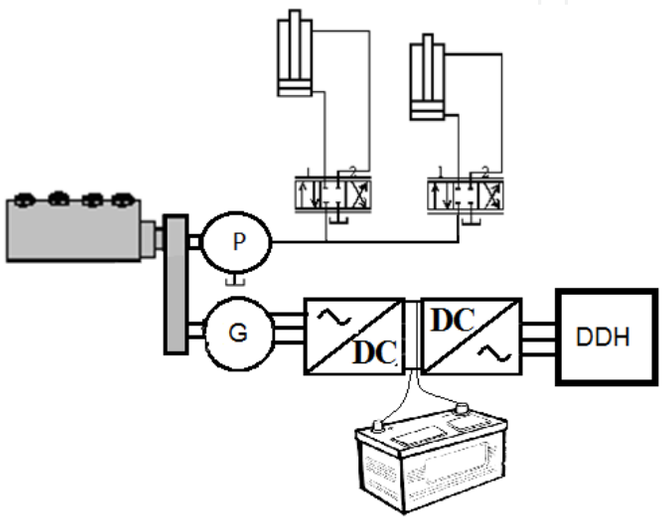

Figure 3. Hybrid proposal for NRMM with DDH.

The next chapter introduces the experimental DDH setup.

2. Description of test setup

The experimental setup uses a speed-controlled electric servo motor drive rotating two hydraulic pumps to directly control the amount of hydraulic oil pumped to the asymmetrical double-acting cylinder MIRO C-10-60/30× 400. The simplified circuit diagram of the experimental test setup is illustrated in Figure 4. The hydraulic pump/motors P_1 and P_2 create an input and output flow that depends on the rotating speed of the servo motor. The oil pressure rises to the required level as determined by the payload. During lowering motion, the potential energy of the payload creates a flow that rotates the hydraulic machine P_1 as a motor and the hydraulic machine P_2 as a pump, and the mechanically connected electric motor acts as a generator, which is controlled by the frequency converter. The speed-controlled generator controls the amount of fluid flow and the position of the payload. The program for the electric drive controls both the electrical and hydraulic sides of the system as there is no conventional valve control.

For easier understanding of the real displacements of the pumps, the following ratios R_A and R_Q will be defined. In this work, the ratio between the cylinder areas is defined by the following equation:

$$R_A = \frac{A_3}{A_1},$$

where $A_3 = A_1 - A_2$ is the cylinder area from the rod side. The diameter of the cylinder piston head is $d_1 = 0.06$ m and $d_2 = 0.03$ m is the diameter of the piston rod, which determines the piston surface areas A_1 and A_2. According to the datasheet, the cylinder stroke is $l = 0.4$ m.

As previously stated, the pump/motors P_1 and P_2 are mounted on the same axis, so their speeds are identical. If the pump leakage is ignored, the ratio of the flow rates R_Q can be produced directly from the displacement of the pump/motors D_1 and D_2.

$$R_Q = \frac{D_2}{D_1}.$$

Figure 4 illustrates the first prototype of the DDH setup with $R_Q \approx 0.63$ and $R_A = 0.75$. To test the concept, the components for this prototype were taken off the shelf.

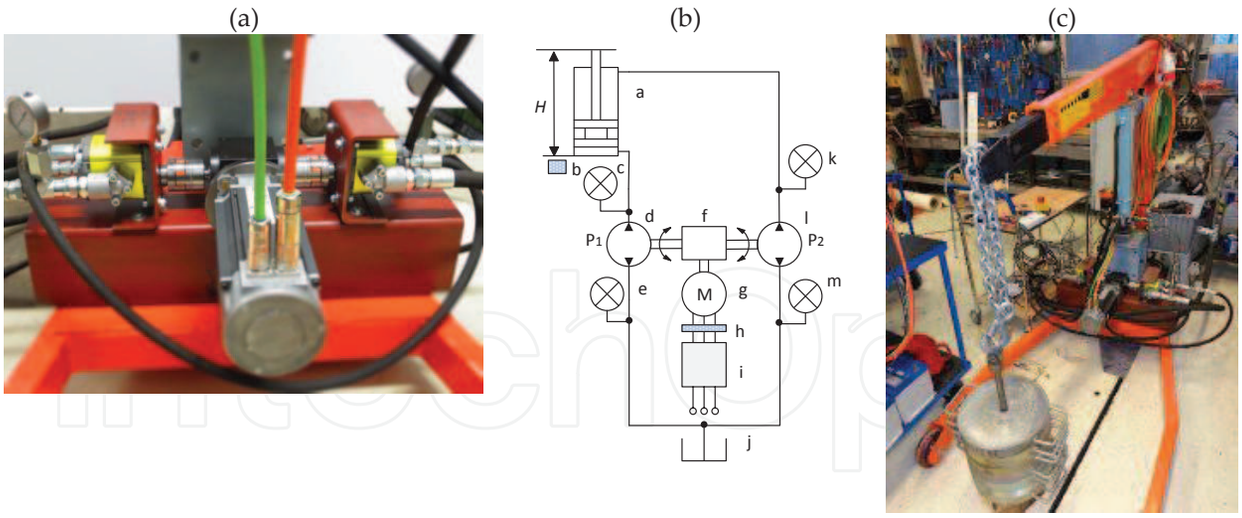

Figure 4. First prototype of the DDH setup: (a) zoom view;(b) the experimental setup consists ofa) a double-acting cylinder, b) wire-actuated encoder, c) pressure sensor, d) reversible gear pump/motor P_1, e) pressure sensor, f) gearbox, g) PMSM motor/generator, h) current sensors, i)frequency converter, j) tank, k) pressure sensor, l) reversible gear pump/motor P_2 and m) pressure sensor in the tank line; (c) the crane is used for the DDH setup as a test platform (side view).

Two XV-2M internal gear pump/motors by Vivoil with displacements of 14.4 and 22.8 cm^3/rev were used, P_2 and P_1, respectively [20]. The position feedback from the motor is given by means of its in-built incremental encoder (4096 pulses per revolution, resolution 14 bits), and read

http://dx.doi.org/10.5772/61793

with the Unidrive SP1406 drive software [21]. It converts the AC power supply from the line and allows the speed of the permanent magnet brushless servo motor, Unimotor 115U2C manufactured by Emerson Control Techniques, to be set, taking advantage of the information obtained by the feedback device fitted to ensure the rotor speed is exactly as demanded [22]. This experimental setup was tested with a payload of 150 kg at motor speed ranges from 300 to 500 rpm. Figure 5 shows an example of measured data for a motor speed of 400 rpm and a payload of 150 kg: speed, torque and pressure.

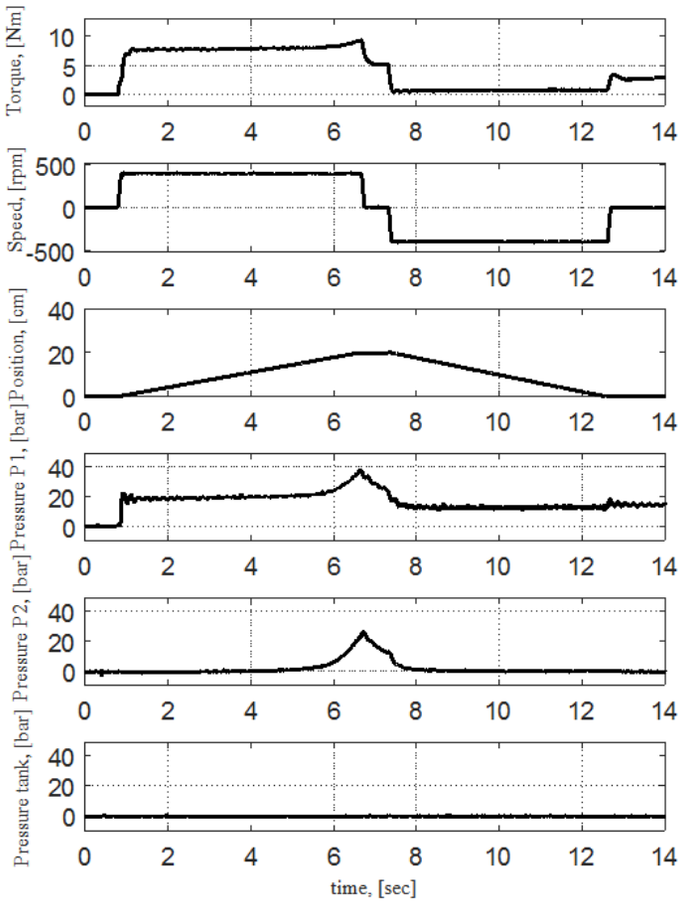

Figure 5. Example of measured data of the first DDH prototype: motor speed, torque, pressure in the pump/motor line P_1 and in the pump/motor line P_2. For a motor speed of 400 rpm and a payload of 150 kg.

In Figure 5, during the lifting, which lasts from 1 to 7 s, the pressure in the pump/motor P_1 is about 2 MPa, which rises by the end to 4 MPa. It is worth remarking that the rise appears to be due to the difference between R_Q and R_A. A similar rise also occurs in the pump/motor line P_2, from atmospheric pressure to 2.6 MPa.

During the lowering, performed from 7 to 13 s, a drop in the pressure from high pressure to about 1 MPa happens. During the lifting, the motor torque is 7 Nm; during the lowering, the torque is around 1 Nm. The pressure in the tank line is close to atmospheric pressure, as it is supposed to be in an open system.

In order to overcome the rise in pressure at the end of the movement and investigate the tankless approach, a new prototype was designed. Figure 6 illustrates the experimental test setup of the second DDH prototype. The system is closed by giving up the tank completely (compare to Figure 2b) and replacing it with a hydraulic accumulator A.

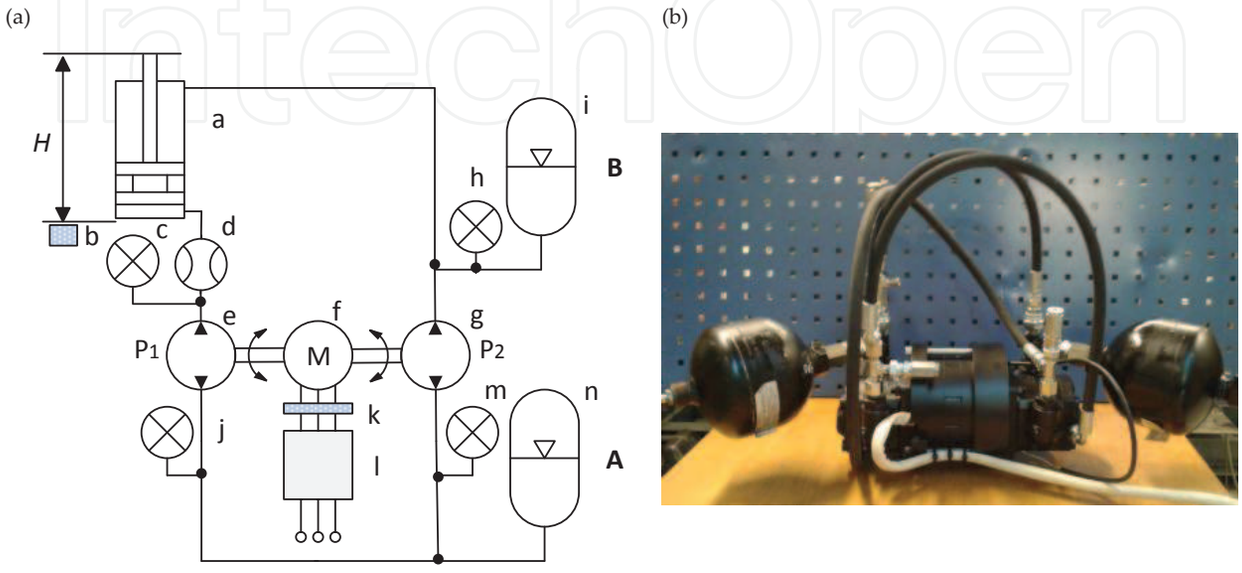

Figure 6. (a) Schematics of the setup of the second DDH prototype: a) double-acting cylinder, b) wire-actuated encoder, c) pressure sensor, d) flow meter,e) reversible gear pump/motor P_1, f) PMSM motor/generator, g) reversible gear pump/motor P_2, h) pressure sensor, i) hydraulic accumulator B, j) pressure sensor in tank line, k) current sensors, l) frequency converter, m) pressure sensor and n) hydraulic accumulator A; (b) photograph of DDH setup.

Within the framework of this work for the second prototype $R_Q \approx 0.73$ and $R_A = 0.75$. It can be seen that the ideal $R_Q = R_A$ was not achieved. Therefore, an accumulator B is added to compensate for the displacement difference between the available pump/motors and cylinder areas.

2.1. Components used

In the second prototype, DDH setup an electric motor, an IndraDyn T MST130A-0250-N torque motor from Bosch Rexroth, is used. The parameters of the electric motor are shown in Table 1.

Rated power	Rated torque	Maximum torque	Nominal speed	Maximum speed	Pole pairs	Torque constant	Voltage constant	Resistance	Inductance
1.2 kW	4.5 Nm	13 Nm	2500 rpm	4000 rpm	10	1.3 Nm/A	0.085 V/ min^{-1}	5.9 Ohm	17.5 mH

Table 1. IndraDyn T MST130A-0250-N parameters [23].

http://dx.doi.org/10.5772/61793

Bosch Rexroth AZMF-12-011U and AZMF-12-008U external gear motors are used as hydraulic pumps/motors. The parameters of the pump/motors are shown in Tables 2 and 3.

Flow rate	Maximum pressure	Leakage-oil pressure	Minimum speed	Maximum speed
11 $\times 10^{-6}$ m^3/rev	25 MPa	0.3 MPa*	500 Nm	3500 rpm

Table 2. Parameters of the AZMF-12-011U hydraulic pump/motor P_1 [24].

Flow rate	Maximum pressure	Leakage-oil pressure	Minimum speed	Maximum speed
8 $\times 10^{-6}$ m^3/rev	25 MPa	0.3 MPa*	500 Nm	4000 rpm

* Short-term pressure during start 1 MPa.

Table 3. Parameters of the AZMF-12-008U hydraulic pump/motor P_2 [24].

Two Parker AD100B20T9A1 diaphragm accumulators are utilized as the initial choices. Table 4 shows the parameters of the hydraulic accumulators.

Capacity (volume)	Maximum pressure
0.001 m^3	200 MPa

Table 4. Parameters of the AD100B20T9A1 hydraulic accumulators A and B.

The pressure was measured with Gems 3100R0400S pressure transducers. The velocity of the cylinder piston was measured with an SGW/SGI wire-actuated encoder by SIKO.

According to the manufacturer, the pump/motors used have an external leakage-oil line with a pressure limitation of 0.3 MPa. During the start, the maximum allowed short-term pressure is 1 MPa. Thus, a detailed investigation of the hydraulic connection of the external leakage line is required.

3. Investigation of the hydraulic connections

This chapter introduces calculations for pump/motor leakage flow in order to identify a suitable connection for the external leakage line. The DDH system can be divided into three separated fluid volumes: the piston side of the cylinders A_1 and the rod side of the cylinders A_3 with the hydraulic accumulator B and the hydraulic accumulator A between the pump/motors. The accumulation of hydraulic fluid in any of these volumes will raise the pressure, as was shown in Figure 5 for the first prototype.

This chapter contains a simple model in which the volumetric efficiency of the pumps $\eta_{v,\,p}$, determines the actual volume produced and the leakage flow of the pump/motor. For simplicity, it is assumed that this efficiency is the same for both pumps/motors. This model is a rough simplification as in reality, the leakage flow is distributed both as internal and external leakage flow [25] and volumetric efficiency varies as a function of the differential pressure and speed. This case study aims to find out how leakages should be controlled so that the system is as insensitive to fluctuations in the volumetric efficiency as possible.

The calculations were performed by determining the change in the volume of fluid during the lifting and lowering with the maximum stroke length of the cylinder l [26]. The volume changes are determined during a single lifting–lowering cycle.

Next, the theoretical flow Q_{Vt}, the actual flow Q_{Vr} and the leakage flow Q_{Vl} for both pumps are determined. It is assumed that the speed of the electric motor is n in rev/s. In this case, the pumps produce theoretical flows of:

$$Q_{\mathrm{Vt1}} = n \cdot D_1, \tag{1}$$

$$Q_{\mathrm{Vt2}} = n \cdot D_2, \tag{2}$$

where D_1 and D_2 are the theoretical pump displacements for the pump/motors P_1 and P_2, respectively.

The actual flows Q_{Vr1} and Q_{Vr2} and leakage flows Q_{Vl1} and Q_{Vl2} in accordance with the volumetric pump efficiency η (D, p) are

$$Q_{\mathrm{Vr1}} = \eta_{\mathrm{V,p}} \cdot n \cdot D_1, \tag{3}$$

$$Q_{\mathrm{Vr2}} = \eta_{\mathrm{V,p}} \cdot n \cdot D_2, \tag{4}$$

$$Q_{\mathrm{Vl1}} = \left(1 - \eta_{\mathrm{V,p}}\right) \cdot n \cdot D_1, \tag{5}$$

$$Q_{\mathrm{Vl2}} = \left(1 - \eta_{\mathrm{V,p}}\right) \cdot n \cdot D_2. \tag{6}$$

During the lifting, the side flow $Q_{Vc1,up}$ of the cylinder A_1 is equal to the actual flow Q_{Vr1} produced by the pump/motor P_1. Theoretical flow Q_{Vt1} leaves the pump/motor P_1 during the lowering from A_3 cylinder's side. Therefore,

http://dx.doi.org/10.5772/61793

$$Q_{\mathrm{Vc1,up}} = Q_{\mathrm{Vr1}}. \tag{7}$$

$$Q_{\mathrm{Vc1,down}} = Q_{\mathrm{Vt1}}. \tag{8}$$

The cylinder losses are assumed to be negligible, so the required flows $Q_{\mathrm{Vc2,up}}$ and $Q_{\mathrm{Vc2,down}}$ are determined as

$$Q_{\mathrm{Vc2,up}} = R_{\mathrm{A}} \cdot Q_{\mathrm{Vr1}} = R_{\mathrm{A}} \cdot \eta_{\mathrm{V,p}} \cdot n \cdot D_1, \tag{9}$$

$$Q_{\mathrm{Vc2,down}} = R_{\mathrm{A}} \cdot Q_{\mathrm{Vt1}} = R_{\mathrm{A}} \cdot n \cdot D_1. \tag{10}$$

It is assumed that the cylinder is moved at a constant velocity v, which can be determined as follows for lifting and lowering, respectively:

$$v = \frac{Q_{\mathrm{Vs1}}}{A_1}, \text{ where } v_{\mathrm{up}} = \frac{Q_{\mathrm{Vr1}}}{A_1}, \; v_{\mathrm{down}} = \frac{Q_{\mathrm{Vt1}}}{A_1}. \tag{11}$$

In this case, the raising (t_{up}) and lowering (t_{down}) times can be calculated by combining Equations (1), (3) and (11):

$$t_{\mathrm{up}} = \frac{l}{v_{\mathrm{up}}} = \frac{l \cdot A_1}{Q_{\mathrm{Vr1}}} = \frac{l \cdot A_1}{\eta_{\mathrm{v,p}} \cdot n \cdot D_1}, \tag{12}$$

$$t_{\mathrm{down}} = \frac{l}{v_{\mathrm{down}}} = \frac{l \cdot A_1}{Q_{\mathrm{Vt1}}} = \frac{l \cdot A_1}{n \cdot D_1}. \tag{13}$$

As was stated earlier, the external leakage line of the pump/motors that are used should be connected to the line under 0.3 MPa. The next section will determine the structure. The least sensitive case will be selected as the system structure. The review will be carried out for a total of four different alternative cases. Figure 7a illustrates Case I, where both the leakage lines are connected to the line with hydraulic accumulator A. In Case II in Figure 7b, both external leakage lines are connected to hydraulic accumulator B. Figure 7c shows Case III, where the external leakage lines of the pump/motors P_2 and P_1 are connected to the line with hydraulic accumulators A and B, respectively. Figure 7d illustrates Case IV, where the external leakage lines of the pump/motors P_1 and P_2 are connected to the lines with hydraulic accumulators A and B, respectively.

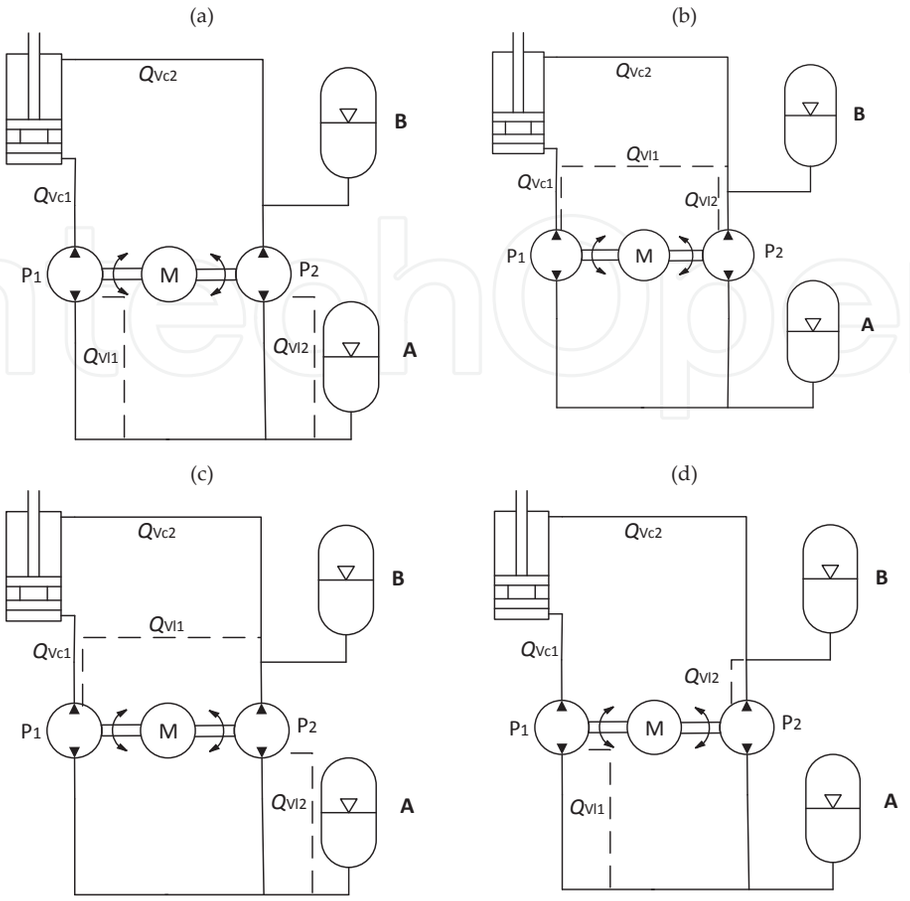

Figure 7. Cases to direct the pump/motor external leakage flows: (a) Case I, (b) Case II, (c) Case III and (d) Case IV.

3.1. Case I

In Case I, during the lifting, the A_3 side of the cylinder should remove flow equal to $Q_{Vc2,up}$, and the pump P_2 is able to remove the theoretical flow of Q_{Vt2}. Thus, during the entire lifting motion, the volume $\Delta V_{up,I}$ can be obtained with Equations (2), (9) and (12):

$$\Delta V_{\mathrm{up,I}} = t_{\mathrm{up}} \cdot \left(Q_{\mathrm{Vc2,up}} - Q_{\mathrm{Vt2}} \right) = l \cdot A_1 \left(R_A - \frac{R_{\mathrm{Q}}}{\eta_{\mathrm{v,p}}} \right). \tag{14}$$

During the lowering, the A_3 chamber of the cylinder should receive the flow of $Q_{Vc2,down}$. The pump/motor P_2 is able to produce the actual flow of Q_{Vr2}. Thus, during the whole cycle in the A_3 chamber of the cylinder, the following difference in volumes $\Delta V_{down,I}$ occurs, which is obtained with Equations (4), (10) and (13):

$$\Delta V_{\mathrm{down,I}} = t_{\mathrm{down}} \cdot \left(Q_{\mathrm{Vr2}} - Q_{\mathrm{Vc2,down}} \right) = l \cdot A_1 \left(\eta_{\mathrm{v,p}} \cdot R_{\mathrm{Q}} - R_{\mathrm{A}} \right). \tag{15}$$

http://dx.doi.org/10.5772/61793

The entire cycle change of volume $\Delta V_{t,I}$ in Case I is:

$$\Delta V_{t,I} = \Delta V_{up,I} + \Delta V_{down,I} = l \cdot A_1 \cdot R_Q \left(\eta_{v,p} - \frac{1}{\eta_{v,p}} \right). \tag{16}$$

3.2. Case II

Figure 7b illustrates Case II, where both of the leakage lines are connected to the line with hydraulic accumulator B and A_3 chamber branch. During the lifting, the chamber A_3 should remove the flow $Q_{Vc2,up}$, as well as the leakage flows of the pumps Q_{Vl1} and Q_{Vl2}. The pump/motor P_2 is able to remove the theoretical flow Q_{Vt2}. In this case, the volume $\Delta V_{up,II}$ is obtained with Equations (2), (5), (6), (9) and (12):

$$\Delta V_{up,II} = t_{up} \cdot \left(Q_{Vc2,n} + Q_{Vl1} + Q_{Vl2} - Q_{Vt2} \right) = l \cdot A_1 \left(R_A + \frac{1 - \eta_{v,p}}{\eta_{v,p}} - R_Q \right). \tag{17}$$

During the lowering, the A_1 chamber of the cylinder should remove the flow $Q_{Vc2,down}$. The pump/motor P_2 is able to provide the flow Q_{Vr2}. In addition, the same line will also have the external leakage flows Q_{Vl1} and Q_{Vl2}. In this case, the change in the volume $\Delta V_{down,II}$ can be obtained with equations (4), (5), (6), (10) and (13):

$$\Delta V_{down,II} = t_{down} \cdot \left(Q_{Vr2} + Q_{Vl1} + Q_{Vl2} - Q_{Vc2,down} \right) = l \cdot A_1 \left(R_Q + 1 - \eta_{v,p} - R_A \right). \tag{18}$$

The entire cycle change of volume $\Delta V_{t,II}$ in Case II is:

$$\Delta V_{t,II} = \Delta V_{up,II} + \Delta V_{down,II} = l \cdot A_1 \left(\frac{1}{\eta_{v,p}} - \eta_{v,p} \right). \tag{19}$$

3.3. Case III

In Case III, the leakage flow of the pump/motor P_2 is connected to the hydraulic accumulator A line and the P_1 leakage flow to the A_3 chamber line of the cylinder, as shown in Figure 7c. During the lifting, the A3 chamber of the cylinder should pump out the flow $Q_{Vc2,up}$ and the pump/motor P_1 the leakage flow Q_{Vl1}, but at the same time the pump/motor P_2 can remove the flow of Q_{Vt2}. Thus, during the whole stroke of the lift, the change in the volume is derived from Equations (2), (5), (9) and (12):

$$\Delta V_{up,III} = t_{up} \cdot \left(Q_{Vc2,up} + Q_{Vl2} - Q_{V2t} \right) = l \cdot A_1 \left(R_A + \frac{1 - \eta_{v,p}}{\eta_{v,p}} - \frac{R_Q}{\eta_{v,p}} \right). \tag{20}$$

During the lowering, the A_3 chamber of the cylinder should provide the flow $Q_{Vc2,down}$. The pump/motor P_2 is able to pump out a flow equal to $Q_{Vr2.}$ In this case, the total volume of $\Delta V_{down,III}$ is obtained with Equations (4), (5), (10) and (13):

$$\Delta V_{down,III} = t_{down} \cdot \left(Q_{Vr2} + Q_{Vl2} - Q_{Vc2,down} \right) = l \cdot A_1 \left(\eta_{v,p} \cdot R_Q + 1 - \eta_{v,p} - R_A \right). \tag{21}$$

The entire cycle volume change $\Delta V_{t,\,III}$ in Case III is:

$$\Delta V_{t,III} = \Delta V_{up,III} + \Delta V_{down,III} = l \cdot A_1 \left(R_Q - 1 \right) \left(\frac{1}{\eta_{v,p}} - \eta_{v,p} \right). \tag{22}$$

3.4. Case IV

In Case IV, the leakage flow from the pump/motor P_1 is directed to the hydraulic accumulator A and the leakage flow of the pump/motor P_2 is directed to the hydraulic accumulator B. During the lifting, A_3 chamber flow of the cylinder $Q_{Vc2,up}$ and leakage flow Q_{Vl2} should be removed by the pump/motor P_2, but the pump/motor P_2 is able to actually pump out the flow of Q_{Vt2}. Thus, during the whole stroke, the change in the volume of the fluid chamber $\Delta V_{up,IV}$ is obtained with Equations (2), (6), (9) and (12):

$$\Delta V_{up,IV} = t_{up} \cdot \left(Q_{Vc2,up} + Q_{Vl2} - Q_{Vt2} \right) = l \cdot A_1 \left(R_A - R_Q \right). \tag{23}$$

During the lowering, the A_3 chamber of the cylinder should pump out the $Q_{Vc2,down}$ volume flow. The required pumping flow rate of P_2 is Q_{Vr2} and the additional leakage flow is Q_{Vl2}. In this case, the change in the volume $\Delta V_{down,IV}$ is obtained with Equations (4), (6), (10) and (13):

$$\Delta V_{down,IV} = t_{down} \cdot \left(Q_{Vr2} + Q_{Vl2} - Q_{Vc2,down} \right) = l \cdot A_1 \left(R_Q - R_A \right). \tag{24}$$

The entire cycle change in the volume $\Delta V_{t,\,IV}$ in Case IV is:

$$\Delta V_{t,IV} = \Delta V_{up,IV} + \Delta V_{down,IV} = 0\ . \tag{25}$$

4. Summary

Four cases of the locations of pump/motor leakages were investigated. The different implementation variants were determined by the changes in the volume of the cylinder as a function

http://dx.doi.org/10.5772/61793

of the volumetric efficiency, and the results are shown in Figure 8. As a result, Case IV appears to be the most independent case [26]. However, this method did not investigate the pressure built up with various payloads. Neither did this investigation consider the practical aspects of realizing such a system. Therefore, the system structure will be investigated further in Matlab Simulink.

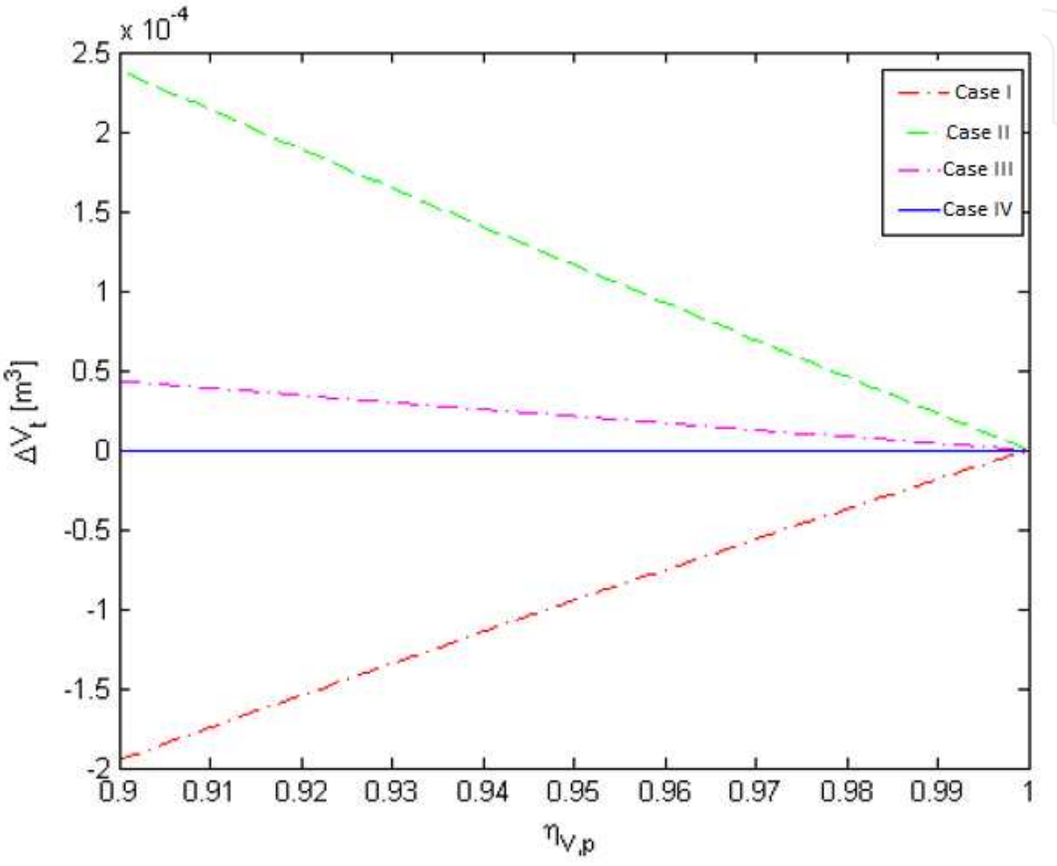

Figure 8. Results of the DDH system with four cases of external leakage connections [26].

5. Simulink modeling

Matlab Simulink R2015a and Simscape SimHydraulics and the SimPowerSystems component library were used for creating the simulation model. The following assumptions were made:

- The effect of temperature on fluid properties is neglected.
- External leakages in the hydraulic pump/motor are neglected. Volumetric efficiency is assumed to be 1.
- Losses in the hydraulic accumulator are ignored.

The simulation model for the test setup (introduced in Figure 2) is shown in Figure 9.

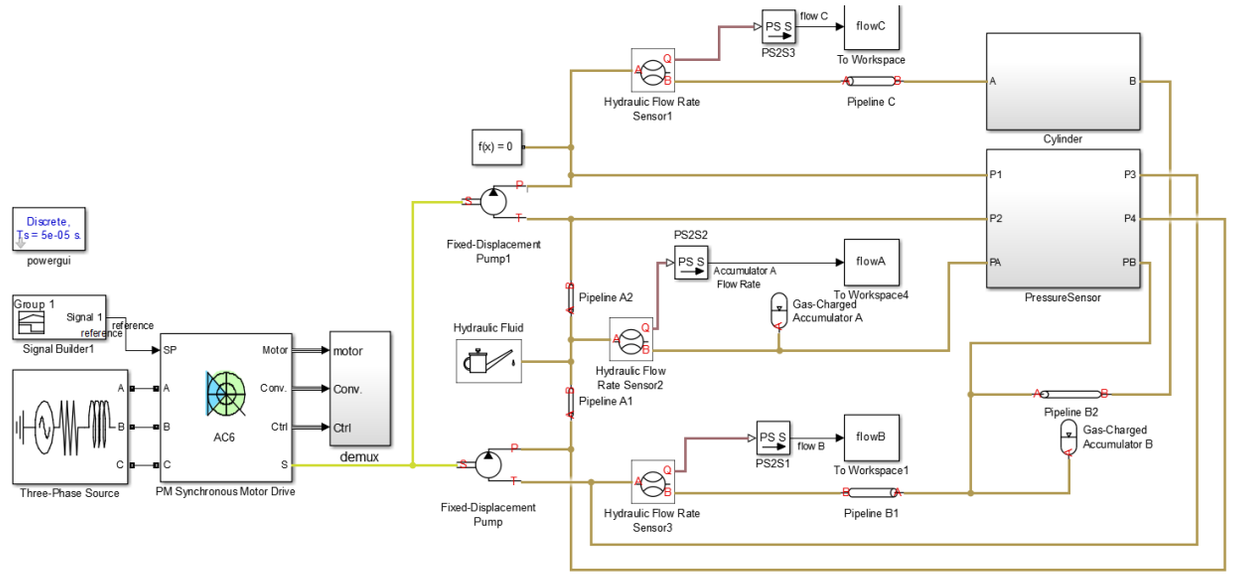

Figure 9. Simulation model of the DDH system.

Figure 10 illustrates the simulation results: reference signal, motor speed and cylinder position. A maximum payload of 150 kg was utilized for the simulation.

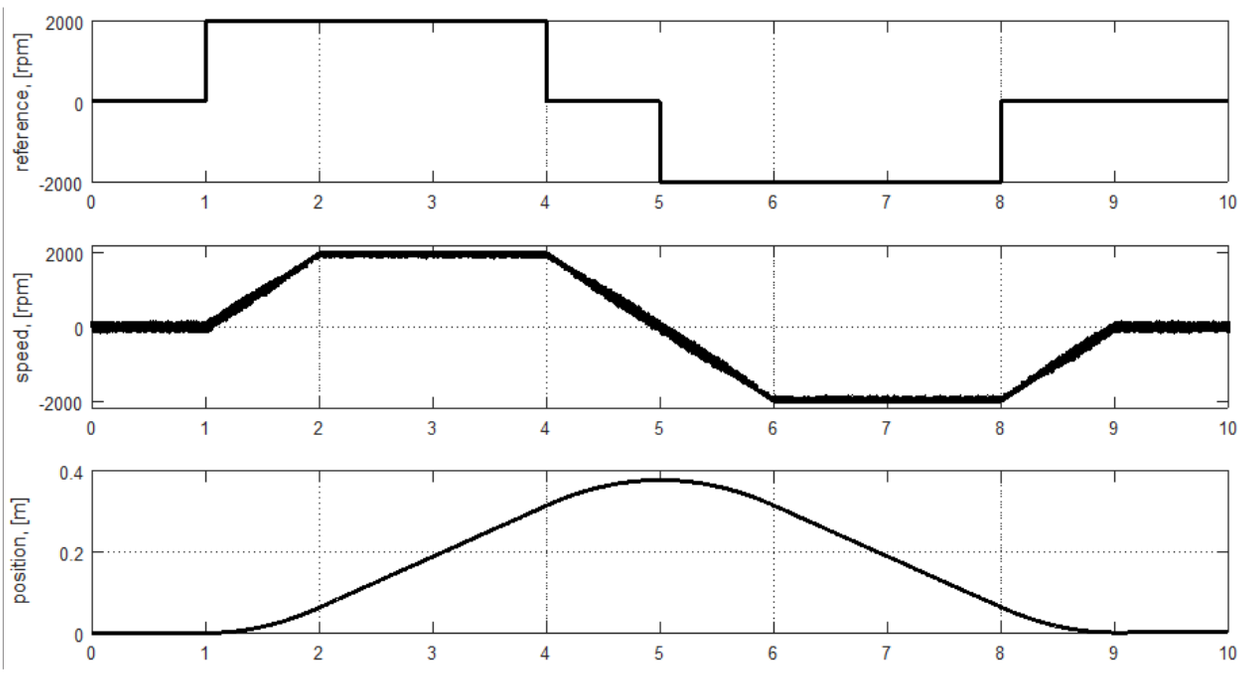

Figure 10. Simulation results of the DDH system: reference signal, motor speed and cylinder position.

The movement of the cylinder is smooth and identical to the first prototype demonstrated in Figure 5. The flows in volume A (the line with accumulator A), B (the line with accumulator B) and C (line between the pump/motor P_1 and the cylinder) are illustrated in Figure 11.

http://dx.doi.org/10.5772/61793

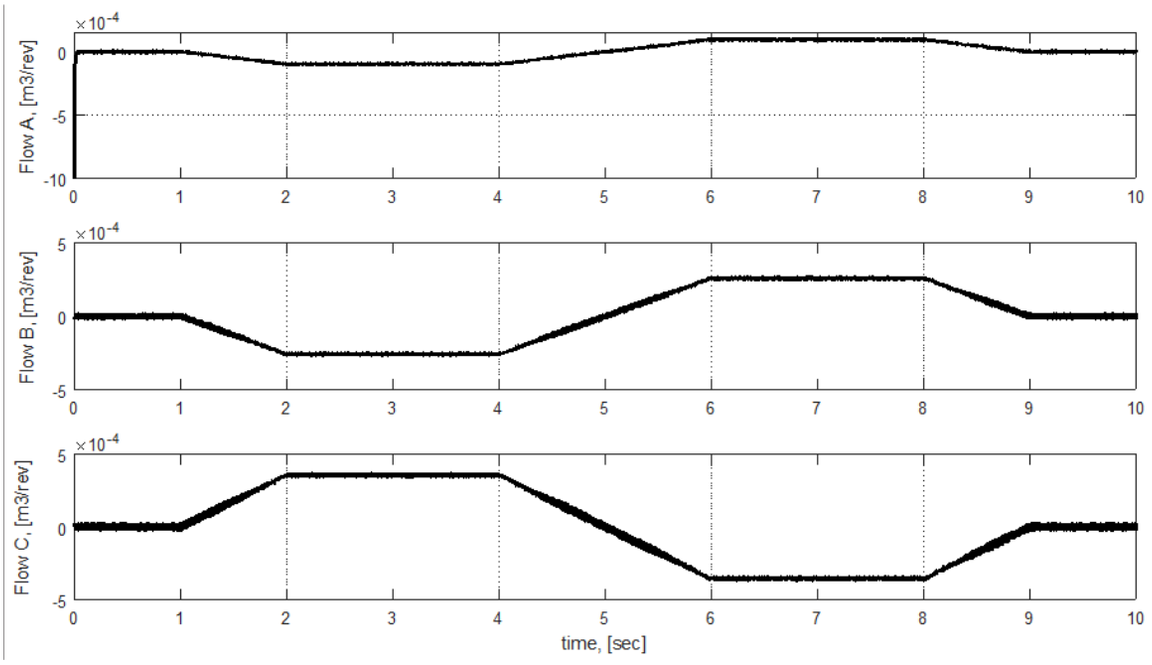

Figure 11. Simulation results of the DDH system: flow in lines A, B and C.

Flows B and C are mirrors of each other, which corresponds to correct behavior. Conversely, flow A has an initial drop which corresponds to sucking in oil from accumulator A during the initial lifting motion.

Figure 12 illustrates the experimental results for two system configurations with hydraulic accumulators: A and A + B. The pressure with accumulator A (red line) configuration goes up to 2.7 MPa, whereas the proposed combination A + B maintains the pressure in the range of 0.7 MPa.

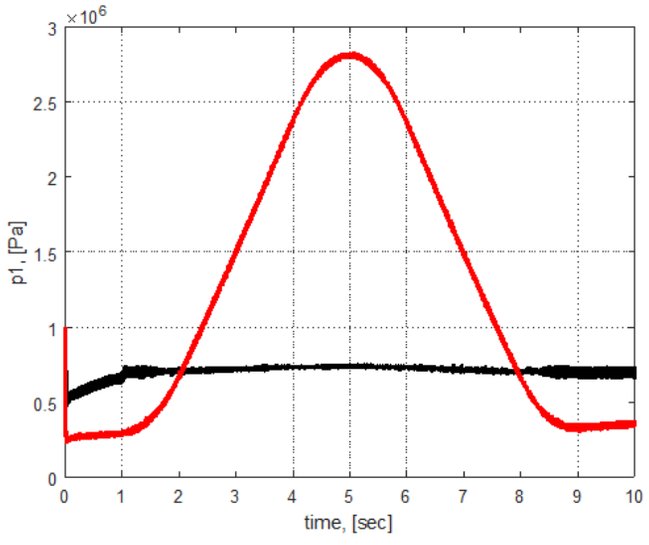

Figure 12. Simulation results of the pressure in the DDH system only with accumulator A (red line) and with accumulators A + B (black line).

The system pressure is illustrated in Figure 13, where p_1 is the P_1 pump/motor pressure, p_3 is the P_2 pump/motor pressure, and p_2, p_4 are the "tank" line pressures (line with accumulator A).

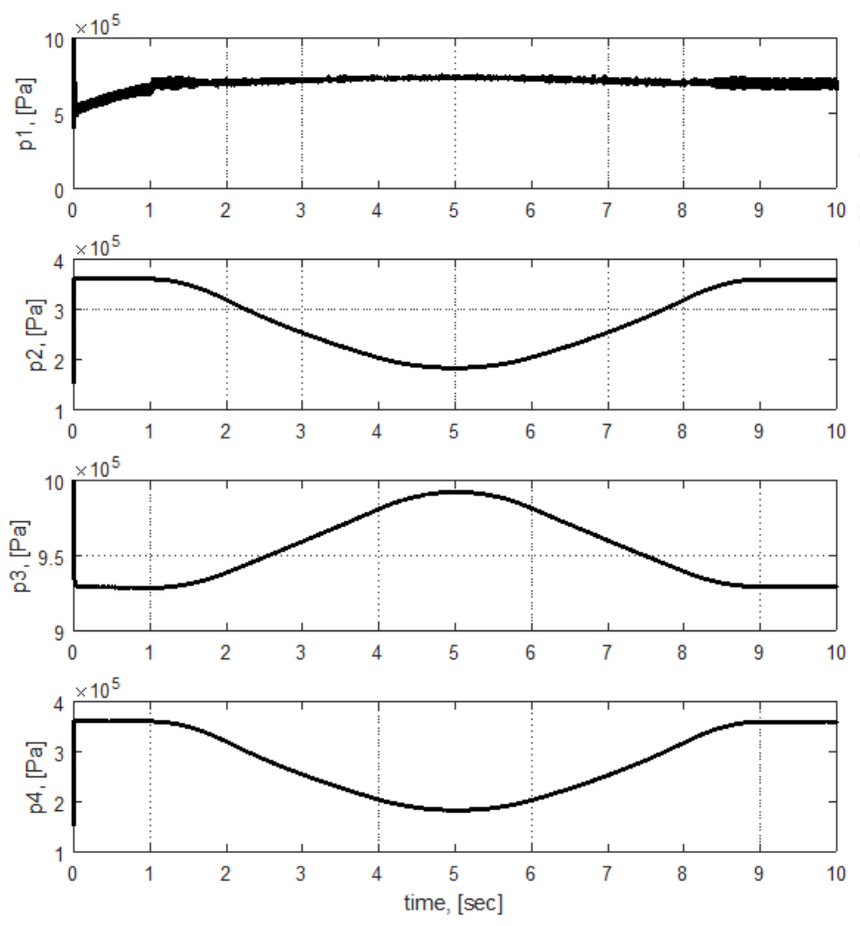

Figure 13. Simulation results of the pressure in the DDH system: p_1 is the P_1 pump/motor pressure, p_3 is the P_2 pump/motor pressure, and p_2, p_4 are the "tank" line pressures (accumulator A).

The pressure p_3 ranges between 0.93 MPa and 1 MPa during the whole lifting–lowering cycle with a maximum payload of 150 kg. The tank pressure (p_2 and p_4) varies between 0.38 MPa and 0.18 MPa. Thus, according to the simulation, Cases II, III and IV do not fulfill the requirements of the leakage line where the maximum allowed constant pressure is 0.3 MPa and in the short term, it is 1 MPa. According to the results shown in Figure 13, from the proposed connection cases in Figure 7, only Case I can be used for the realization of the DDH setup, where both external leakage lines are connected to line A (accumulator A).

6. Experimental investigation

The essential parameters, such as currents, voltage, pressure, flow and height, were measured from the DDH setup. The location of the utilized sensors is illustrated in Figure 4. The

http://dx.doi.org/10.5772/61793

experimental efficiencies and energies of the DDH test setup system for lifting movements were calculated as shown below:

$$\eta_{\text{up\_tot}} = \frac{E_{\text{pot}}}{E_{\text{mech}}}, \tag{26}$$

where E_{pot} is the potential energy of the payload

$$E_{\text{pot}} = mgH, \tag{27}$$

where m is the mass of the payload in kg and g is a gravitational constant in m/s^2. H is the position of the cylinder piston in m.

E_{mech} is the energy of the shaft and is calculated as the integral of the power at the shaft (P_{shaft}).

$$P_{\text{shaft}} = T\Omega, \tag{28}$$

where P_{shaft} is the output energy of the shaft in W, T is the motor torque in Nm and Ω is the angular speed in rad/s. A motor control algorithm was utilized to measure the angular speed and estimate the motor torque.

The output energy of the hydraulic part E_{hydr} is calculated as the integral of the output hydraulic power:

$$P_{\text{hydr}} = pv_cA, \tag{29}$$

where p is the pressure in Pa, v_c is the velocity of the cylinder piston in m/s and A is the cross area of the cylinder piston in m^2.

Depending on the operating point of a hydraulic pump/motor unit in its performance curve, the relationship between the flow and hydraulic losses in a system varies significantly. During the lifting, the hydraulic pump/motor unit operates as a pump. The input energy of the pump is mechanical energy and the output is hydraulic energy. Figure 14 presents an example of a Sankey diagram for the measured losses and efficiencies of the DDH system.

In Figure 14, hydro-mechanical losses equal 33.4%. Hydro-mechanical losses include shaft and hydraulic losses. Hydraulic losses in DDH systems are composed of pipe friction losses and other fittings, entrance and exit losses and losses from changes in the pipe size resulting from a reduction in the diameter, pump/motors and cylinder losses. The overall cylinder efficiency is mostly dependent on the frictional losses encountered by the piston and the rod during its stroke. Frictional losses depend on the pressure difference across the seal, sliding velocity, seal material, temperature, time, wear and direction of the movement. Measured electrical machine

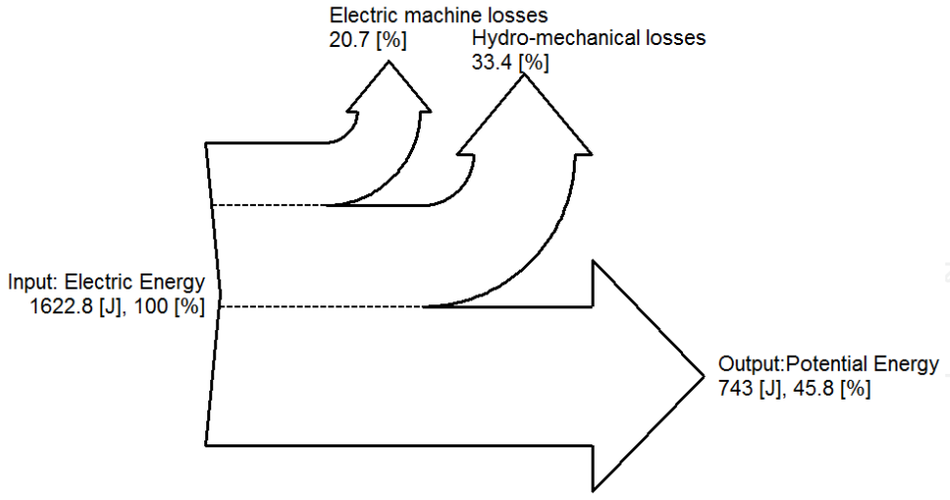

Figure 14. Measured Sankey diagram of the DDH with a motor speed of 400 rpm and a payload of 150 kg (the efficiency of the frequency converter is not included) [19].

losses are 20.7%. Electrical machine losses are composed of the following elements: stator and rotor resistive losses, iron losses, additional losses and mechanical losses. Mechanical losses include friction in the motor bearings. Bearing losses depend on the shaft speed, bearing type, properties of the lubricants and the load. The converter losses take place mostly in the semiconductor switches and in the auxiliary power systems. In this study, the losses of the frequency converter are not included.

It was challenging to create the DDH test setup due to the asymmetrical double-acting cylinder used and the difficulty of finding matching displacements of the pump/motors in order to fulfill $R_Q = R_A$. Moreover, another challenge was the location of the hydraulic accumulators and external leakage pump/motor lines. The Sankey diagrams showed that electrical machine losses are in second place after the dominant hydro-mechanical losses. Taking pressure balancing into consideration, the hydro-mechanical losses in the system will be reduced in the second DDH prototype.

7. Conclusion

This paper described a DDH setup and its potential for applicability to NRMMs. It investigates the compensation of pump/motor displacement for an asymmetrical double-acting cylinder and the location of hydraulic accumulators and external leakage pump/motor lines. The review was carried out for four different alternative cases. The mathematical model used in the review suggested Case IV as the least sensitive case. Further investigations were performed in Matlab Simulink. According to the simulations, Cases II, III and IV did not fulfill the requirements of a leakage line where the maximum allowed constant pressure was 0.3 MPa and, in the short term, it was 1 MPa. Therefore, only Case I can be used for the realization of the DDH setup, in which both external leakage lines are connected to line A (accumulator A).

The experimental tests demonstrated that direct-driven hydraulics (DDH) has the advantage of a fully self-contained electrohydraulic actuator, which combines the high power density of hydraulics and the accuracy of an electric motor. The measured energy efficiency of the DDH varies by up to 46% with the direction of the motion of the cylinder and the motor speed. As the Sankey diagram showed, the hydro-mechanical losses dominate in the original DDH setup. As expected, with regard to the efficiency of the DDH setup, the weak link in the chain is found in the losses of the hydro-mechanical components of the system. Therefore, further studies are required on the improvement of DDH.

Acknowledgements

The research was enabled by the financial support of ArcticWell project (Academy of Finland) and internal funding at the Department of Engineering Design and Production at Aalto University.

Author details

Tatiana A. Minav[1*], Jani E. Heikkinen[2] and Matti Pietola[1]

*Address all correspondence to: tatiana.minav@aalto.fi

1 Department of Engineering Design and Production, School of Engineering, Aalto University, Finland

2 Independent researcher, http://orcid.org/0000-0002-5991-7580, Helsinki, Finland

References

[1] Tier 4 Emission Standards for Nonroad Diesel Engines, online, https://www.dieselnet.com/standards/us/nonroad.php#tier4.

[2] Liukkonen, M., Lajunen, A., Suomela, J. Comparison of different buffering topologies in FC-hybrid non-road mobile machineries. At the 7th IEEE Vehicle Power and Propulsion Conference, Chicago, September 6–9, 2011. Chicago 2011.

[3] Wang, T. et al. An energy-saving pressure-compensated hydraulic system with electrical approach. ieee/asme transactions on mechatronics, vol. 19, no. 2, april 2014 Mech., 2013.

[4] Bifeng, Y., Tao, G., Shengji, L.,. Investigate on the combustion and emission characteristics of small non-road diesel engine fueled with bio-diesel, In 2012 (ISDEA), 2012, pp. 852–856.

[5] Skinner, J., Smith, A., Frischemeoer, S., Holland, M. Advancements in hydraulic systems for more electric aircraft. Proceedings of MEA 2015 Conference, Toulouse, France, February 2015.

[6] Youzhe, J., Song, P., Li, G., Zhanlin, W., Lihua, Q. Pressure loop control of pump and valve combined EHA based on FFIM. The Ninth International Conference on Electronic Measurement & Instruments, 2009.

[7] Zhang, Q., Li, B. Feedback linearization PID control for electro-hydrostatic actuators, at 2nd International Conference on Artificial Intelligence, Management Science and Electronic Commerce (AIMSEC), 2011, p. 358 - 361, DOI: 10.1109/AIMSEC. 2011.6010249

[8] Liang, B., Li, Y., Zhang, Z. Research on Simulation of Aircraft Electro-Hydrostatic Actuator Anti-Skid Braking System (ICMTMA), 2011.

[9] Altare, G., Vacca, A., Richter, C. A novel pump design for an efficient and compact electro-hydraulic actuator. IEEE Aerospace Conference, 2014 IEEE, 2014, pp. 1–12.

[10] Ahn K. K., Nam D.N.C.., Jin M.,. Adaptive backstepping control of an electrohydraulic actuator. IEEE/ASME Transactions on Mechatronics, Vol. 19, No. 3, June 2014.

[11] Mini-Motion Package (MMP), [online] http://www.kybfluidpower.com/Mini_Motion_Package.html.

[12] AC Servo Motor Driven Hydraulic Pump Control System, [online] http://www.yuken.co.uk/long_cat/%5BK%5D/816-817.pdf.

[13] Daher, N., Ivantysynova, M. Electro-hydraulic energy-saving power steering systems of the future. Proceedings of the 7th FPNI PhD Symposium on Fluid Power, 27-30 June 2012, Reggio Emilia, Italy.

[14] Michel, S., Weber, J., Electrohydraulic compact-drives for low power applications considering energy-efficiency and high inertial loads. 2012. Fluid Power and Motion Control FPMC 2012 conference, Bath, UK, p.93-109

[15] Michel, S., et al. Energy-efficiency and thermo energetic behavior of electrohydraulic compact drives, at 9th International Fluid Power Conference (IFK), 24 - 26 March 2014, Aachen, Germany.

[16] Busquets, E., Ivantysynova M. Temperature prediction of displacement controlled multi-actuator machines. Int. J. of Fluid Power, Jan., 2014.

[17] Busquets, E. An investigation of the cooling power requirements for displacement-controlled multi-actuator machines, M.Sc thesis, Purdue university, 2013.

[18] Minav, T., Bonato, C., Sainio, P., Pietola, M. Direct driven hydraulic drive, at 9th International Fluid Power Conference (IFK), 24 - 26 March 2014, Aachen, Germany.

[19] Minav, T.A., Bonato, C., Sainio, P., Pietola, M. Efficiency of direct driven hydraulic drive for non-road mobile working machines, at 2014 International Conference on Electrical Machines (ICEM), 2-5 September 2014, Berlin, Germany, pp. 2431–2435.

[20] Vivoil motor, Data Sheet: reversible motor - series XV, http://www.vivoil.com/files/xm_en/xm201.pdf, visited on September 8, 2013.

[21] Emerson Control Techniques Unidrive SP1406 drive, http://www.emersonindustrial.com, visited on September 8, 2013.

[22] Emerson Control Techniques Unimotor 115U 2C, http://www.emersonindustrial.com/en-en/documentcenter/ControlTechniques/Brochures/unimotor_fm_product_data.pdf, visited on 1 September, 2013.

[23] Bosch Rexroth Indradyn T Torque motors. [online]. http://www.boschrexroth.com/dcc/content/internet/en/pdf/PDF_p146807_en.pdf.

[24] Bosch Rexroth AZMF External gear motors. [online]. www.boschrexroth.com.

[25] Kauranne, H., Kajaste, J., Vilenius, M. Hydraulitekniikka, Helsinki: Sanoma Pro Oy, 2013. 496 p. ISBN 978-962-63-0707-7.

[26] Kiesi, M. Suorasähkökäyttöisen hydraulijärjestelmän paineakun valinta ja mitoitus, Bachelor Thesis, Aalto University, 2014.

IntechOpen